

## ORIGINAL ARTICLE

# Differential Diagnosis among Alzheimer's Disease, Mild Cognitive Impairment, and Normal Subjects Using Resting-State fMRI Data Extracted from Multi-Subject Dictionary Learning Atlas: A Deep Learning-Based Study

Farzad Alizadeh <sup>1,2</sup>, Hassan Homayoun <sup>1</sup>, Seyed Amir Hossein Batouli <sup>3</sup>, Maryam Noroozian <sup>4</sup>, Forough Sodaie <sup>1,2</sup>, Hanieh Mobarak Salari <sup>1</sup>, Anahita Fathi Kazerooni <sup>5</sup>, Hamidreza Saligheh Rad <sup>1,2\*</sup> 

<sup>1</sup> Quantitative MR Imaging and Spectroscopy Group, Research Center for Molecular and Cellular Imaging, Tehran University of Medical Sciences, Tehran, Iran

<sup>2</sup> Department of Medical Physics and Biomedical Engineering, School of Medicine, Tehran University of Medical Sciences, Tehran, Iran

<sup>3</sup> Department of Neuroscience and Addiction Studies, School of Advanced Technologies in Medicine, Tehran University of Medical Sciences, Tehran, Iran

<sup>4</sup> Cognitive Neurology and Neuropsychiatry Division, Department of Psychiatry, Tehran University of Medical Sciences, Tehran, Iran

<sup>5</sup> Department of Radiology, Perelman School of Medicine, University of Pennsylvania, Philadelphia, Pennsylvania, USA

\*Corresponding Author: Hamidreza Saligheh Rad  
Email: [hamid.saligheh@gmail.com](mailto:hamid.saligheh@gmail.com)

Received: 25 October 2021 / Accepted: 25 December 2021

## Abstract

**Purpose:** A powerful imaging method for evaluating brain patches is resting-state functional Magnetic Resonance (rs-fMRI) Imaging, in which the subject is at rest. Artificial Neural Networks (ANN) are one of the several Alzheimer's Disease (AD) analysis and diagnosis methods used in this study. We investigate ANNs' ability to diagnose AD using rs-fMRI data.

**Materials and Methods:** The acquisition of functional and structural magnetic resonance imaging was applied for 15 AD, 17 mild cognitive impairment, and ten normal healthy participants. Time series of blood oxygen level-dependent were extracted from the multi-subject dictionary learning brain atlas after pre-processing. This study develops a one-dimensional Convolutional Neural Network (CNN) using extracted signals of the functional atlas for differential diagnosis of AD.

**Results:** Applying the proposed method to rs-fMRI signals for classifying three classes of Alzheimer's patients resulted in overall accuracy, F1-score, and precision of 0.685, 0.663, and 0.681, respectively. Using 39 regions in the brain and proposing a quite simple network than most of the available deep learning-based methods are the main advantages of this model.

**Conclusion:** rs-fMRI signal recognition based on a functional atlas with the application of a deep neural network has a pattern recognition capability that can make a differential diagnosis with an acceptable level of accuracy and precision. Therefore, deep neural networks can be considered as a tool for the early diagnosis of AD.

**Keywords:** Alzheimer's Disease; Resting-State Functional Magnetic Resonance Imaging; Blood-Oxygen-Level-Dependent Signal; Artificial Neural Network; Deep Learning.

## 1. Introduction

Alzheimer's Disease (AD) is a very burdensome disease, the burden of which is increasing more dramatically than any other disease in recent years. The number of people with AD is expected to be more than 70 million worldwide [1]. Since there is no single straightforward test for AD detection, various approaches and methods should be applied to help make a diagnosis. These approaches include obtaining a medical and family history, psychiatric history, and history of cognitive and behavioral changes, blood tests, and brain imaging [2]. Despite the various approaches, there are still caveats to distinguishing between these diagnoses.

Neuroimaging techniques such as Electroencephalogram (EEG) [3], Single Photon Emission Computed Tomography (SPECT) [4], Positron Emission Tomography (PET) [5], Magnetoencephalography (MEG) [6], structural Magnetic Resonance Imaging (sMRI) [7], and Functional Magnetic Resonance Imaging (fMRI) [8] can be applied to diagnose AD. These techniques enable detailed examination of pathophysiologic and neurodegenerative processes in AD [9]. MRI is a non-invasive method and provides high spatial resolution. So, it is widely used in diagnosing AD.

Brain functions and hemodynamic response investigations have proved helpful in diagnosing neurodegenerative disorders [10]. Resting-State Functional Magnetic Resonance Imaging (rs-fMRI) has been under investigation in several different approaches in AD. The amplitude of low-frequency fluctuation [11], the fractional amplitude of low-frequency fluctuations [12], regional homogeneity [13], independent component analysis [14], and functional connectivity [15] are some of the important approaches which can be used in the healthy or diseased brain.

Various artificial intelligence-based techniques are available for classification tasks. The Support Vector Machine (SVM) in the machine learning method is the most popularly applied to AD research [16]. Deep Learning (DL) is a subset of artificial intelligence, and it was born with the emergence of powerful graphics processing units [17]. Several DL architectures such as Convolutional Neural Networks (CNN), Recurrent Neural Networks (RNN), Autoencoders (AE), and Deep Belief Network (DBN) can classify a variety of disorders [18]. Studies using DL to classify AD have used a range of data, including sMRI, rs-fMRI, Diffusion Tensor Images (DTI), PET data, and genomics data [19].

Many algorithms based on the structural or functional brain changes can detect AD or Mild Cognitive Impairment (MCI). They vary from simple volumetric measures or a complex mathematical description of the shape difference in Regions of Interest (ROIs) [20] to voxel-level analysis and modeling [21]. Several pieces of review research have explored the ability of DL which applied rs-fMRI to classify neurological disorders [22, 23, 24]. In [25], a combination of rs-fMRI and score of mini-mental examination for 331 participants was employed to build an ensemble of algorithms for AD classification. The significance of this research is the selection of an appropriate brain atlas that provides results nearly two times superior to the chance level while using a simple artificial neural network.

## 2. Materials and Methods

### 2.1. Participants

Fifteen diagnosed AD subjects, seventeen diagnosed MCI subjects, and ten Normal Control (NC) subjects participated in this study. They were 52 to 90 years of age in each group. All subjects were screened and excluded if they had dementia with Lewy bodies, Pick, and Vascular dementia. Moreover, those with diabetes, cancer, hypertension, severe Anemia, Parkinson's, and other severe chronic medical disorders were excluded. Moreover, subjects with intellectual disability, a history of substance abuse, or severe head trauma were excluded. Written informed consent was obtained. Table 1 presents the demographics of our dataset. An expert cognitive neurologist diagnosed the participants as AD, MCI, or NC based on the mini-mental state exam and structured clinical interview of the national institute of neurological and communicative disorders and Alzheimer's disease and related disorders association criteria. Participants had acquired in Roozbeh hospital (Tehran) and their imaging data in the national brain-mapping laboratory (Tehran) from 2018 to 2021. Tehran university of medical sciences gave the ethical code of IR.TUMS.MEDICINE.REC.1399.675 for this research.

**Table 1.** dataset demographic: Age-Gender distribution of participants in this study

Diagnosis	Male/Female	Age (Standard deviation)
AD	5/10	78.86 (7.72)
MCI	3/14	71.31 (7.79)
NC	5/5	67.60 (4.56)

## 2.2. Structural Image Acquisition

All the participants were scanned with a Siemens MAGNETOM Prisma 3.0 Tesla scanner. The following parameters were applied during a Magnetization Prepared Rapid Gradient Echo (MPRAGE) sequence: Repetition Time (TR)/ Echo time (TE)/ Inversion Time (TI) = 1840/ 3.55/ 800 milliseconds, flip angle =  $7^\circ$ , the Field Of View (FOV) =  $220 \times 220$  millimeters, slices per slab = 176, echo spacing = 8.4 milliseconds, voxel size =  $0.9 \times 0.9 \times 0.9$  millimeters, multi-slice mode = sequential, bandwidth = 190 Hertz per pixel.

## 2.3. Functional Image Acquisition

The following parameters were applied during the resting-state image acquisitions, which were collected with single-shot full k-space Echo-Planar Imaging (EPI) with TR = 3000 milliseconds, TE = 30 milliseconds, slice thickness = 3 millimeters, voxel size =  $2.8 \times 2.8 \times 3.0$  millimeters, number of slices = 45. All subjects were supine during the acquisition process and instructed to keep their eyes open, stare at the fixation cross, and not think of a specific matter.

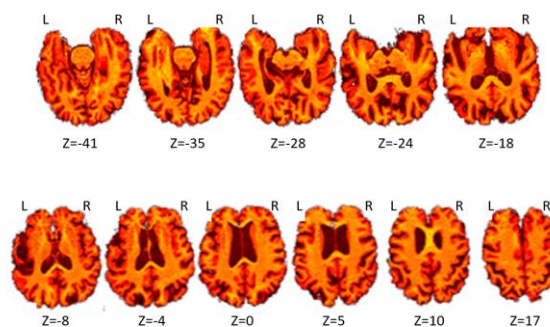
## 2.4. Pre-Processing

Image pre-processing was carried out with the Oxford FMRIB Software Library (FSL) version 5.0 [26]. Firstly, intra-cranial regions of MPRAGE MRI scans were extracted with the FSL Brain Extraction Tool (BET). Figure 1 shows the output of BET for a given case. The FSL Linear Registration Tool (FLIRT) was performed an affine registration with a standard parameter configuration.

The first volume of the rs-fMRI data of the same subject co-registered to anatomical image counterpart through the boundary-based registration algorithm. Finally, the full 3D registrations with MNI152 standard space were applied. In Figure 2, sagittal, coronal, and axial views of a sample of each class are shown.

Three rotational and three translational estimation measures were calculated. Moreover, the estimation of absolute and the relative head motion was calculated. These estimations are presented in Figure 3. As the head motion has a substantial effect on functional brain studies [27], we have checked subjects head motion after correction by FSL MCFLIRT, and since there was no subject with absolute head motion more than 3 millimeters or relative

head motion more than 1.5 millimeters in any of the x, y or z-direction, no one excluded.



**Figure 1.** Intra-cranial regions of MPRAGE MRI scan of a 71 years old male AD patient extracted with the BET

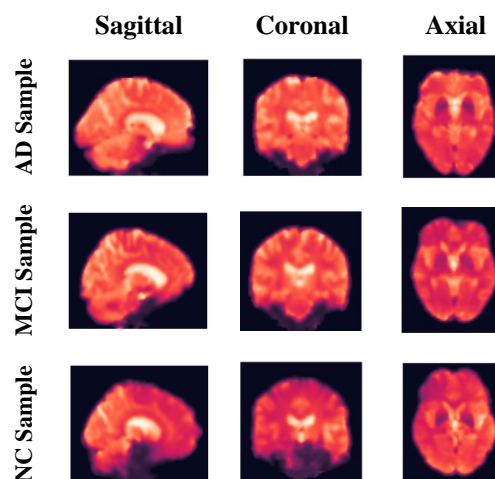


**Figure 2.** Three views of the three samples, each of them belonging to a specific class in our dataset (AD, MCI, or NC)

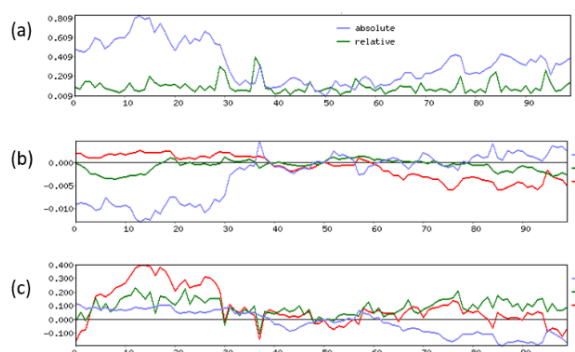


**Figure 3.** Head motion correction estimation: a) mean displacement (millimeters). b) mean rotation (radians) c) mean translation (millimeters)

## 2.5. Brain Regions of Interest

This study examines Multi-Subject Dictionary Learning (MSDL) atlas to segment the brain's spontaneous activity. This atlas segments the brain into 39 parcels. The parcellation is based on learning simultaneously latent spatial maps and the corresponding brain activity time series of 20 healthy subjects scanned twice in a resting-state [28]. Figure 4 provides the segmented ROIs in cut coordination of (2, -1, 20) within the MSDL atlas.

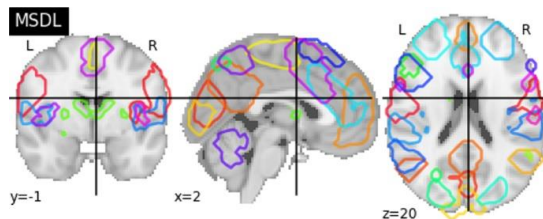


**Figure 4.** The MSDL atlas was applied to segment the spontaneous brain activity in this study

## 2.6. Signal Augmentation

In the case of small data sets such as medical images, the overfitting problem is expected. This issue can be resolved by increasing the sample size. We divided our Blood Oxygen Level Dependent (BOLD) time series into shorter time series utilizing the sliding window technique. In this scenario, a time series with a length of 100 breaks down into 10 time series with 30.

## 2.7. Deep Neural Network

High-performance computers lead to the emergence of models with multiple levels of abstraction and millions of compute nodes, which allows for characterization with a high degree of accuracy [29]. These models are collectively called DL methodologies [30]. CNN [31], AE [32], and

DBNs [33] are the most common DL models for brain image studies. DL is used for brain image analysis in several applications, including neurodegenerative disease diagnosis such as AD [34].

The deeper an Artificial Neural Network (ANN) is, the more abstract features are achievable. Nevertheless, when the available data is limited, deepening the network does not guarantee better performance. Thus, the suitable number of hidden layers determination is crucial. There is an input layer and three sequential hidden layers in our one-Dimensional Convolution Neural network (1D CNN); each consists of a convolutional layer followed by rectified linear unit activation. The output layer corresponds to the number of classes (Table 2).

## 2.8. Reproducibility

The training process is initialized with random weights so that the results may be different for a given model on the same dataset. In order to gain a reliable accuracy measure, we repeated the train-test procedure ten times, and the result of this calculation plus their average are presented in the result section.

## 2.9. Validation Scheme

The validation data set has an essential role in the validation of ANNs' performance. So, it should be selected appropriately. The most reliable selection of validation data set in the case of rare medical data is one-case-leave-out validation. It means the training process is not included any of the test data. Some previous studies had achieved a false high amount of accuracy because they had ignored this vital selection. Cross-validation is the most common technique to compensate lack of labeled data. We repeated the train-test process 42 times.

**Table 2.** Details of the 1D CNN architecture are presented in the present paper

	Layer	Feature map	Stride	Kernel Size
<b>Input Layer</b>	Input	39		
	Convolution	8	1	3
<b>Hidden Layers</b>	Rectified Linear Unit	8	1	3
	Convolution	16	1	3
	Rectified Linear Unit	15	1	3
	Convolution	32	1	3
	Rectified Linear Unit	32	1	3
	Global Average Pooling	32		
<b>Output Layer</b>	Softmax	3		

### 3. Results

In this section, the obtained results are presented based on the validation scheme discussed in the previous section. Ten-repeated calculated accuracy and its average are reported in Figure 5.

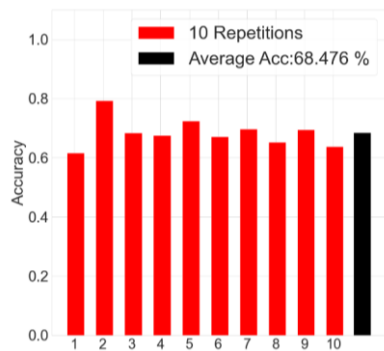


**Figure 5.** Results: accuracy scores of 10 repetitions and its average

In order to evaluate the effectiveness of the proposed model, different evaluation indicators were applied. It includes the accuracy, F1-score, precision, specificity, and sensitivity. These metrics are elicited from the confusion matrix, which is represented in Table 3.

**Table 3.** Confusion matrix of employed 1D CNN model

Confusion Matrix	Predicted Labels		
	AD	MCI	NC
True Labels AD	12	1	2
True Labels MCI	6	11	0
True Labels NC	2	3	5

These measures are calculated based on Equations 1 to 5 [35]. In the case of AD versus MCI, True Positive (TP) and True Negative (TN) are the numbers of cases that are correctly identified as MCI and AD, respectively. False Positive (FP) and False Negative (FN) are the numbers of subjects that are incorrectly identified as MCI and AD, respectively. In the case of AD versus NC, TP and TN are the numbers of cases that are correctly identified as NC and AD, respectively. FP and FN are the numbers of subjects that are incorrectly identified as NC and AD, respectively. In the case of MCI versus NC, TP and TN are the numbers of cases that are correctly identified as NC and MCI, respectively. FP and FN are the numbers of subjects that are incorrectly identified as NC and MCI, respectively.

$$Accuracy = \frac{TP + TN}{TP + TN + FP + FN} \quad (1)$$

$$F1 - score = \frac{2TP}{2TP + FP + FN} \quad (2)$$

$$Precision = \frac{TP}{TP + FP} \quad (3)$$

$$Specificity = \frac{TN}{TN + FP} \quad (4)$$

$$Sensitivity = \frac{TP}{TP + FN} \quad (5)$$

The macro, micro, and weighted averaging of F1-score and precision calculation result are provided in Table 4.

Specificity and sensitivity criteria are calculated in a binary scheme, and they are presented in Table 5.

**Table 4.** F1-score and precision calculated in macro, micro, and weighted averaging scheme

	F1_score	Precision
<b>Macro Averaging</b>	0.654	0.683
<b>Micro Averaging</b>	0.667	0.667
<b>Weighted Averaging</b>	0.663	0.681

**Table 5.** Results for specificity and sensitivity

	Specificity	Sensitivity
<b>AD V.s MCI</b>	0.923	0.647
<b>AD V.s NC</b>	0.857	0.714
<b>MCI V.s NC</b>	1	0.625

### 4. Discussion

AD is a degenerative disease in various symptoms and stages, from invisible brain changes to changes that affect memory and ultimately physical impairment. Several different approaches and methods are employed to diagnose AD because there is no one simple test to do that.

On the one hand, the radio frequency nature of MRI makes it intrinsically non-invasive; and on the other hand, it provides images with higher spatial resolution than other modalities such as PET, SPECT, and EEG. So, it could be the best option among all imaging modalities to diagnose neurodegenerative diseases like AD.

It seems that employing additional data such as age, sex, and apolipoprotein E information to the rs-fMRI can elevate the results; in [36], they applied these data

beside rs-fMRI and achieved sensitivity and specificity of 94% and 96% utilizing an AE network, respectively.

Employing a single slice of the 3D or 4D data as its original label would be unreliable. In other words, for example, a single slice of structural data of an AD patient should not be considered as an AD-labeled image. Some studies ignore this and achieve high accuracy with the abovementioned 2D images when shuffled for train/test procedures. Although sliced structural data may contain spatial information, in the case of rs-fMRI data, slicing means ignoring the time dimension since they are inherently time series. The high accuracies of 96.86%, 97.92%, 97.63%, 91.85%, and 97.5% that have been acquired in [37], [38], [39], [40], and [41] indicate that the training data includes images of adjacent slices of the test set.

One of the main characteristics of the DL methodology is the elimination of feature selection steps, which is common in ML. Accuracy of 86% in [42] is attained when they extracted the features with information gain and ReliefF methods. In [43], the rs-fMRI connectivity matrix was constructed, using the optimal features extracted from the graph measures resulted in an accuracy of 88.4% for the 3-group classification. Also, the binary classification of AD vs. others, MCI vs. others, and NC vs. others resulted in 97.5%, 72.0%, and 87.3%, respectively. In [8], discriminant correlation analysis and sequential feature collection methods were used for feature selection, and an accuracy of 67% was obtained. Multi-voxel pattern analysis (MVPA) is a statistical method applied for AD classification. In [44], the accuracy of 81.9% was achieved

through the MVPA method. Table 6 illustrates the methods and results of studies on AD diagnosis.

MR imaging can be used to detect brain AD-caused alterations in the diseased brain with structural or functional images. Since the BOLD signals reflect the cerebral metabolic rate of oxygen consumption, it could take a role as a searchlight to find brain regions' metabolic rate alterations. Some studies suggest that high accuracy is achievable when sMRI data is used in a DL network [45, 46, 47]. Results of this research and others' [48, 49] proved that using resting-state imaging has also achieved significant outcomes. The accuracy metric of similar studies in which structural or functional MRI data were used in a Deep Learning (DL) method for AD classification is presented in Table 7.

Our proposed model's Accuracy to the Chance Level ratio (ACC/CL) is more than other mentioned studies where rs-fMRI data is applied. The accuracy to the chance level ratio of other studies based on rs-fMRI and sMRI is demonstrated in Figure 6. The confusion matrix showed that the model could not accurately diagnose MCI Vs. AD since it predicted 6 MCI cases as AD among all 17 MCIs.

There were forty-two cases in three classes of the disease in our study, which is the smallest sample size compared to others. It should be considered that the other studies brought to this comparison which employed rs-fMRI, are two-classes classification problems, but in our case, it is a three-classes problem with an accuracy chance

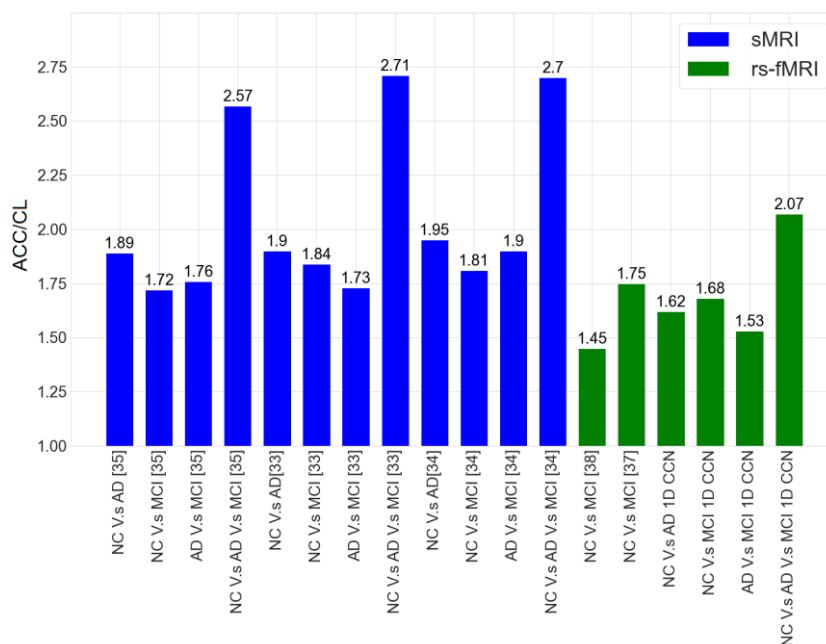


Figure 6. The accuracy to the chance level ratio for similar studies

**Table 6.** Other studies' input, methods and results

Ref.	Input Data	Sample size	Method	Results
[36]	age, sex, genes, and apolipoprotein E + rs-fMRI	MCI: 91 NC: 79	Feature extraction & AE	Accuracy: not reported Sensitivity: 94% Specificity: 96%
[37]	rs-fMRI (2D slices)	AD: 28 NC: 15	2D CNN	AD vs NC accuracy :96.86%
[42]	numerical and categorical data of MRI, PET, genetic data	CN:617, MCI:886, Dementia: 348	2D CNN	Accuracy: 86% Sensitivity: 87% Specificity: 97%
[38]	rs-fMRI (2D slices)	AD: 25 EMCI: 25 LMCI: 25 MCI: 13 NC: 25	2D CNN	Multi-class:97.92% AD vs others: 94.97% EMCI vs others: 91.8% LMCI vs others: 90.50% NC vs others: 91.73% SMC vs others: 100%
[43]	Rs-fMRI connectivity matrix	AD: 45 MCI: 89 NC: 34	ML (Network based statistics)	Multi-class: 88.4 %. AD vs others: 97.5% MCI vs others: 72.0% NC vs others: 87.3%
[39]	rs-fMRI (2D slices)	AD: 29 EMCI: 46 LMCI: 39 NC: 55 SMC: 25	2D CNN	6-group acc: 97.63% AD vs others: 94.97% EMCI vs others: 95.64% LMCI vs others: 95.89% NC vs others: 98.34% SMC vs others: 94.55%
[40]	MRI (2D slices)	AD: 300 MCI: 300 NC: 300	2D CNN	3-group accuracy: 91.85% AD vs MCI: 93.89% MCI vs NC: 91.67% AD vs NC: 98.33 % Average Sen: 96.26% Average Specificity:92.96%
[41]	MRI (2D slices) & rs-fMRI (2D slices)	rs-fMRI: AD: 52 MCI: 131 NC: 92 MRI: AD: 211 MCI: 774 NC: 91	2D CNN	Multi-class accuracy: 97.5%
[8]	Combination of rs-fMRI and sMRI	AD: 34 MCI-C: 25 MCI-NC: 69 NC: 49	ML (SVM)	3-group acc: Acc: 67%
[42]	frequency distribution-based index of FC in default mode network	AD: 26 MCI: 19 NC: 20	MVPA	AD vs MCI in ADNI data set accuracy: 81.9% AD vs MCI for their data set accuracy: 43.1%.

level of 0.33. We calculate each previous study's ACC/CL to compare a two-class problem with a three-class problem. It is represented in the last column of [Table 7](#).

Using 39 regions in the brain and providing a simple network architecture are the main advantages of the proposed method. Moreover, the dictionary learning-based brain

**Table 7.** The accuracy metric of different studies

Ref. number	Input Data	Sample size	DL method	Accuracy	ACC/CL	
[47]	sMRI	AD=200 MCI=411 NC=232	SAE <sup>1</sup> & CNN	NC vs. AD	0.947	1.89
				NC vs. MCI	0.864	1.72
				AD vs. MCI	0.881	1.76
				NC vs. AD vs. MCI	0.850	2.57
[45]	sMRI	AD=755 MCI=755 NC=755	AE & CNN	NC vs. AD	0.954	1.90
				NC vs. MCI	0.921	1.84
				AD vs. MCI	0.868	1.73
				NC vs. AD vs. MCI	0.895	2.71
[46]	sMRI	AD=70 MCI=70 NC=70	AE & CNN	NC vs. AD	0.976	1.95
				NC vs. MCI	0.908	1.81
				AD vs. MCI	0.950	1.9
				NC vs. AD vs. MCI	0.891	2.70
[48]	rs-fMRI	MCI=31 NC=31	DAE <sup>2</sup>	NC vs. MCI	0.726	1.45
[49]	rs-fMRI	MCI=52 NC=48	SAE <sup>3</sup>	NC vs. MCI	0.875	1.75
<b>proposed CNN</b>	<b>rs-fMRI</b>	<b>AD=15 MCI=17 NC=10</b>	<b>1D CNN</b>	<b>NC vs. AD NC vs. MCI AD vs. MCI NC vs. AD vs. MCI</b>	<b>0.809 0.842 0.766 0.685</b>	<b>1.62 1.68 1.53 2.07</b>

<sup>1</sup>SAE: Sparse Autoencoder; <sup>2</sup>DAE: Denoising Autoencoder; <sup>3</sup>SAE: Sparse Autoencoder

atlas is proved to be considered a standard map in functional brain studies.

## 5. Conclusion

We proposed a 1D CNN model for AD classification, which is fed by rs-fMRI BOLD signals. Results proved that it could be helpful for the early detection of this burdensome disorder. We have used a functional atlas to extract the desired data. In addition, there is no need for feature extraction and feature selection in our proposed model, which are essential in machine learning-based classification methods. The performance of our proposed 1D CNN is much more than the chance level; this means that the employed CNN model is learnable with BOLD signals of AD.

Extracting the desired signals from other brain regions may lead to getting the premier results. So, other atlases should be examined. Having a small sample of data was the main limitation of this study. The algorithm would

achieve superior results by further externally validating data from various institutions on a large scale.

## Acknowledgments

This research has been supported by Tehran University of Medical Sciences & Health Services grant number 45447. The authors would like to express special thanks to the National Brain Mapping Laboratory (Tehran, Iran) which gave us services to acquire images.

## References

- 1- Eric McDade and Randall J Bateman, "Stop Alzheimer's before it starts." *Nature News*, Vol. 547 (No. 7662), p. 153, (2017).
- 2- Keith A Johnson *et al.*, "Appropriate use criteria for amyloid PET: a report of the Amyloid Imaging Task Force, the Society of Nuclear Medicine and Molecular Imaging, and the Alzheimer's Association." *Journal of Nuclear Medicine*, Vol. 54 (No. 3), pp. 476-90, (2013).

- 3- Marjolein MA Engels, Cornelis J Stam, Wiesje M van der Flier, Philip Scheltens, Hanneke de Waal, and Elisabeth CW van Straaten, "Declining functional connectivity and changing hub locations in Alzheimer's disease: an EEG study." *BMC neurology*, Vol. 15 (No. 1), pp. 1-8, (2015).
- 4- Varvara Valotassiou, George Angelidis, Dimitrios Psimadas, Ioannis Tsougos, and Panagiotis Georgoulas, "In the era of FDG PET, is it time for brain perfusion SPECT to gain a place in Alzheimer's disease imaging biomarkers?" *European Journal of Nuclear Medicine and Molecular Imaging*, Vol. 48 (No. 4), pp. 969-71, (2021).
- 5- Cathleen Haense, Karl Herholz, WJ Jagust, and Wolf-Dieter Heiss, "Performance of FDG PET for detection of Alzheimer's disease in two independent multicentre samples (NEST-DD and ADNI)." *Dementia and geriatric cognitive disorders*, Vol. 28 (No. 3), pp. 259-66, (2009).
- 6- David López-Sanz, Noelia Serrano, and Fernando Maestú, "The role of magnetoencephalography in the early stages of Alzheimer's disease." *Frontiers in neuroscience*, Vol. 12p. 572, (2018).
- 7- Samaneh Kazemifar et al., "Spontaneous low frequency BOLD signal variations from resting-state fMRI are decreased in Alzheimer disease." *PloS one*, Vol. 12 (No. 6), p. e0178529, (2017).
- 8- Seyed Hani Hojjati, Ata Ebrahimzadeh, and Abbas Babajani-Feremi, "Identification of the early stage of Alzheimer's disease using structural MRI and resting-state fMRI." *Frontiers in neurology*, Vol. 10p. 904, (2019).
- 9- Rik Ossenkoppele et al., "Associations between tau, A $\beta$ , and cortical thickness with cognition in Alzheimer disease." *Neurology*, Vol. 92 (No. 6), pp. e601-e12, (2019).
- 10- Axel Montagne, Daniel A Nation, Judy Pa, Melanie D Sweeney, Arthur W Toga, and Berislav V Zlokovic, "Brain imaging of neurovascular dysfunction in Alzheimer's disease." *Acta neuropathologica*, Vol. 131 (No. 5), pp. 687-707, (2016).
- 11- Ying Han et al., "Frequency-dependent changes in the amplitude of low-frequency fluctuations in amnesic mild cognitive impairment: a resting-state fMRI study." *Neuroimage*, Vol. 55 (No. 1), pp. 287-95, (2011).
- 12- Yongxia Zhou, Fang Yu, Timothy Q Duong, and Alzheimer's Disease Neuroimaging Initiative, "White matter lesion load is associated with resting state functional MRI activity and amyloid PET but not FDG in mild cognitive impairment and early Alzheimer's disease patients." *Journal of Magnetic Resonance Imaging*, Vol. 41 (No. 1), pp. 102-09, (2015).
- 13- Yong Liu et al., "Regional homogeneity, functional connectivity and imaging markers of Alzheimer's disease: a review of resting-state fMRI studies." *Neuropsychologia*, Vol. 46 (No. 6), pp. 1648-56, (2008).
- 14- Timo Tuovinen et al., "The effect of gray matter ICA and coefficient of variation mapping of BOLD data on the detection of functional connectivity changes in Alzheimer's disease and bvFTD." *Frontiers in human neuroscience*, Vol. 10p. 680, (2017).
- 15- Angela Tam et al., "Common effects of amnesic mild cognitive impairment on resting-state connectivity across four independent studies." *Frontiers in aging neuroscience*, Vol. 7p. 242, (2015).
- 16- Benoît Magnin et al., "Support vector machine-based classification of Alzheimer's disease from whole-brain anatomical MRI." *Neuroradiology*, Vol. 51 (No. 2), pp. 73-83, (2009).
- 17- Ian Goodfellow, Yoshua Bengio, and Aaron Courville, *Deep learning*. MIT press, (2016).
- 18- Mufti Mahmud, M Shamim Kaiser, T Martin McGinnity, and Amir Hussain, "Deep learning in mining biological data." *Cognitive Computation*, Vol. 13 (No. 1), pp. 1-33, (2021).
- 19- Janani Venugopalan, Li Tong, Hamid Reza Hassanzadeh, and May D Wang, "Multimodal deep learning models for early detection of Alzheimer's disease stage." *Scientific Reports*, Vol. 11 (No. 1), pp. 1-13, (2021).
- 20- Olivier Colliot et al., "Discrimination between Alzheimer disease, mild cognitive impairment, and normal aging by using automated segmentation of the hippocampus." *Radiology*, Vol. 248 (No. 1), pp. 194-201, (2008).
- 21- Geraldo F Busatto et al., "A voxel-based morphometry study of temporal lobe gray matter reductions in Alzheimer's disease." *Neurobiology of aging*, Vol. 24 (No. 2), pp. 221-31, (2003).
- 22- Mamoon Rashid, Harjeet Singh, and Vishal Goyal, "The use of machine learning and deep learning algorithms in functional magnetic resonance imaging—A systematic review." *Expert Systems*, Vol. 37 (No. 6), p. e12644, (2020).
- 23- Ali Nawaz et al., "A Comprehensive Literature Review of Application of Artificial Intelligence in Functional Magnetic Resonance Imaging for Disease Diagnosis." *Applied Artificial Intelligence*, pp. 1-19, (2021).
- 24- Longhai Li Wutao Yin, Fang-Xiang Wu, "Deep learning for brain disorder diagnosis based on fMRI images." *Neurocomputing*, Vol. 469pp. 332-45, (2022).
- 25- Nguyen Thanh Duc, Seungjun Ryu, Muhammad Naveed Iqbal Qureshi, Min Choi, Kun Ho Lee, and Boreom Lee, "3D-deep learning based automatic diagnosis of Alzheimer's disease with joint MMSE prediction using resting-state fMRI." *Neuroinformatics*, Vol. 18 (No. 1), pp. 71-86, (2020).
- 26- Mark Jenkinson, Christian F Beckmann, Timothy EJ Behrens, Mark W Woolrich, and Stephen M Smith, "Fsl." *Neuroimage*, Vol. 62 (No. 2), pp. 782-90, (2012).

- 27- Koene RA Van Dijk, Mert R Sabuncu, and Randy L Buckner, "The influence of head motion on intrinsic functional connectivity MRI." *Neuroimage*, Vol. 59 (No. 1), pp. 431-38, (2012).
- 28- Gaël Varoquaux, Alexandre Gramfort, Fabian Pedregosa, Vincent Michel, and Bertrand Thirion, "Multi-subject dictionary learning to segment an atlas of brain spontaneous activity." in *Biennial International Conference on information processing in medical imaging*, (2011): Springer, pp. 562-73.
- 29- Hassan Khastavaneh and Hossein Ebrahimpour-Komleh, "Representation Learning Techniques: An Overview." in *The 7th International Conference on Contemporary Issues in Data Science*, (2019): Springer, pp. 89-104.
- 30- Li Deng and Dong Yu, "Deep learning: methods and applications." *Foundations and trends in signal processing*, Vol. 7 (No. 3-4), pp. 197-387, (2014).
- 31- Rikiya Yamashita, Mizuho Nishio, Richard Kinh Gian Do, and Kaori Togashi, "Convolutional neural networks: an overview and application in radiology." *Insights into imaging*, Vol. 9 (No. 4), pp. 611-29, (2018).
- 32- Min Chen, Xiaobo Shi, Yin Zhang, Di Wu, and Mohsen Guizani, "Deep features learning for medical image analysis with convolutional autoencoder neural network." *IEEE Transactions on Big Data*, (2017).
- 33- Manjit Kaur and Dilbag Singh, "Fusion of medical images using deep belief networks." *Cluster Computing*, Vol. 23 (No. 2), pp. 1439-53, (2020).
- 34- Yechong Huang, Jiahang Xu, Yuncheng Zhou, Tong Tong, Xiahai Zhuang, and Alzheimer's Disease Neuroimaging Initiative, "Diagnosis of Alzheimer's disease via multi-modality 3D convolutional neural network." *Frontiers in neuroscience*, Vol. 13p. 509, (2019).
- 35- Hassan Homayoun and Hossein Ebrahimpour-Komleh, "Automated segmentation of abnormal tissues in medical images." *Journal of Biomedical Physics & Engineering*, Vol. 11 (No. 4), p. 415, (2021).
- 36- Haibing Guo and Yongjin Zhang, "Resting state fMRI and improved deep learning algorithm for earlier detection of Alzheimer's disease." *IEEE Access*, Vol. 8pp. 115383-92, (2020).
- 37- Saman Sarraf and Ghassem Tofighi, "Deep learning-based pipeline to recognize Alzheimer's disease using fMRI data." in *2016 future technologies conference (FTC)*, (2016): IEEE, pp. 816-20.
- 38- Farheen Ramzan *et al.*, "A deep learning approach for automated diagnosis and multi-class classification of Alzheimer's disease stages using resting-state fMRI and residual neural networks." *Journal of medical systems*, Vol. 44 (No. 2), pp. 1-16, (2020).
- 39- Yosra Kazemi and Sheridan Houghten, "A deep learning pipeline to classify different stages of Alzheimer's disease from fMRI data." in *2018 IEEE Conference on Computational Intelligence in Bioinformatics and Computational Biology (CIBCB)*, (2018): IEEE, pp. 1-8.
- 40- Ciprian D Billones, Olivia Jan Louville D Demetria, David Earl D Hostallero, and Prospero C Naval, "DemNet: a convolutional neural network for the detection of Alzheimer's disease and mild cognitive impairment." in *2016 IEEE region 10 conference (TENCON)*, (2016): IEEE, pp. 3724-27.
- 41- Saman Sarraf, Danielle D Desouza, John AE Anderson, and Cristina Saverino, "MCADNNet: Recognizing stages of cognitive impairment through efficient convolutional fMRI and MRI neural network topology models." *IEEE Access*, Vol. 7pp. 155584-600, (2019).
- 42- Daniel Stamate *et al.*, "Applying deep learning to predicting dementia and mild cognitive impairment." in *IFIP International Conference on Artificial Intelligence Applications and Innovations*, (2020): Springer, pp. 308-19.
- 43- Ali Khazaei, Ata Ebrahimzadeh, and Abbas Babajani-Feremi, "Application of advanced machine learning methods on resting-state fMRI network for identification of mild cognitive impairment and Alzheimer's disease." *Brain imaging and behavior*, Vol. 10 (No. 3), pp. 799-817, (2016).
- 44- Keiichi Onoda *et al.*, "Can a resting-state functional connectivity index identify patients with Alzheimer's disease and mild cognitive impairment across multiple sites?" *Brain connectivity*, Vol. 7 (No. 7), pp. 391-400, (2017).
- 45- Adrien Payan and Giovanni Montana, "Predicting Alzheimer's disease: a neuroimaging study with 3D convolutional neural networks." *arXiv preprint arXiv:1502.02506*, (2015).
- 46- Ehsan Hosseini-Asl, Georgy Gimelfarb, and Ayman El-Baz, "Alzheimer's disease diagnostics by a deeply supervised adaptable 3D convolutional network." *arXiv preprint arXiv:1607.00556*, (2016).
- 47- Ashish Gupta, Murat Ayhan, and Anthony Maida, "Natural image bases to represent neuroimaging data." in *International conference on machine learning*, (2013): PMLR, pp. 987-94.
- 48- Heung-Il Suk, Chong-Yaw Wee, Seong-Whan Lee, and Dinggang Shen, "State-space model with deep learning for functional dynamics estimation in resting-state fMRI." *Neuroimage*, Vol. 129pp. 292-307, (2016).
- 49- Chenhui Hu, Ronghui Ju, Yusong Shen, Pan Zhou, and Quanzheng Li, "Clinical decision support for Alzheimer's disease based on deep learning and brain network." in *2016 IEEE International Conference on Communications (ICC)*, (2016): IEEE, pp. 1-6.